Soft Janus particles: Ideal building blocks for template-free fabrication of two-dimensional exotic nanostructures

ARTICLE *in* SOFT MATTER · JUNE 2014

Impact Factor: 4.03 · DOI: 10.1039/c4sm00765d · Source: PubMed

3 AUTHORS, INCLUDING:

Zhan-Wei Li
Chinese Academy of Sciences
10 PUBLICATIONS **90** CITATIONS
SEE PROFILE

Zhao-Yan Sun
Chinese Academy of Sciences
106 PUBLICATIONS **697** CITATIONS
SEE PROFILE

Soft Matter

PAPER

Soft Janus particles: ideal building blocks for template-free fabrication of two-dimensional exotic nanostructures†

Cite this: *Soft Matter*, 2014, **10**, 5472

Zhan-Wei Li,[a] Zhong-Yuan Lu[b] and Zhao-Yan Sun*[a]

Received 7th April 2014
Accepted 25th April 2014

DOI: 10.1039/c4sm00765d

www.rsc.org/softmatter

The design and fabrication of two-dimensional (2D) well-ordered nanostructures by a facile and effective strategy remain a major scientific and technological challenge, hitherto achieved mainly through the aid of interfaces or substrates with an ordered arrangement. Here we introduce a new concept in achieving template-free fabrication of diverse 2D ordered nanostructures by utilizing anisotropic characteristics of soft triblock Janus particles. Our numerical investigation demonstrates how particle softness and controllable directional attraction interplay to generate a number of fascinating non-close-packed 2D nanostructures and even three-dimensional (3D) vesicles. These non-close-packed nanostructures are of great interest for scientific reasons and lead to promising applications in soft nanotechnology and biotechnology.

1 Introduction

Two-dimensional (2D) well-ordered colloidal nanostructures are highly desired in many applications, such as optics, photonics, sensing, and surface patterning.[1–5] Various strategies have been successfully developed for the fabrication of 2D colloidal nanostructures, including colloidal lithography and the self-assembly of mono-sized colloids on planar substrates or at an air–water interface.[2–9] However, for most of these fabrication methods, it is necessary to prepare a large area of masks, templates, or substrates with complex geometries and properties, which sometimes may not be readily available.

As a unique and emerging type of patchy particles,[10–12] Janus particles with special anisotropic feature represent a new class of building blocks for the fabrication of hierarchical nanostructures.[13–21] Granick and co-workers showed that the 2D Kagome lattice can be realized using triblock Janus particles if an accurate Janus balance is chosen.[22–24] Moreover, soft Janus colloidal crystal films have been successfully fabricated at an air–water interface.[25] Recent studies also suggested that the thin-film materials with soft and deformable properties have more promising applications in novel soft-electronic and optical devices.[26,27] Therefore, fabricating 2D colloidal nanostructures possessing combined characteristics of softness, asymmetry, and regularity, by a facile template-free nanofabrication technique, is a much desired and challenging goal in materials science.

Herein, we introduce a new concept in achieving template-free fabrication of diverse 2D nanostructures by utilizing the deformable and anisotropic characteristics of soft triblock Janus particles. These particles are spherical and symmetrically decorated with two opposite repulsive patches separated by an attractive middle band, in contrast to the Janus particle used in ref. 22. This design of building blocks easily enables the self-assembly of soft Janus particles to form various 2D ordered nanostructures without the aid of any interfaces or substrates, due to the synergistic effects of particle deformability and energetically favorable side-by-side alignment of soft triblock Janus particles. More importantly, the deformability of soft triblock Janus particles will further expand the limited selection of attainable close-packed structures from the self-assembly of hard colloidal spheres mostly induced by the minimization of entropy.[22] The soft triblock Janus particles in our simulations may be experimentally realized as triblock Janus micelles,[13,17,28,29] Janus microgels,[30] Janus dendrimers,[31,32] and Janus hyperbranched polymers[33] with the attractive middle bands characterized by hydrophobic interactions or hydrogen bond interactions.

The simulations are performed in three-dimensions (3D), but we mainly focus on how to obtain various 2D ordered nanostructures. By properly tuning the Janus balance and the strength of attraction between attractive middle bands, soft triblock Janus particles can spontaneously self-assemble into a number of fascinating 2D ordered non-close-packed (ncp) and

[a]*State Key Laboratory of Polymer Physics and Chemistry, Changchun Institute of Applied Chemistry, Chinese Academy of Sciences, Changchun 130022, China. E-mail: zysun@ciac.ac.cn*

[b]*Institute of Theoretical Chemistry, State Key Laboratory of Theoretical and Computational Chemistry, Jilin University, Changchun 130023, China*

† Electronic supplementary information (ESI) available: The relation between α_{11}^{A} and G, the self-assembly diagram of soft triblock Janus particles, typical self-assembled nanostructures for larger system sizes, the comparison of the radial distribution functions $g(r)$ of 2D sh-ncp arrays and hcp arrays, and the potential energy E *versus* the adhesion energy G. See DOI: 10.1039/c4sm00765d

close-packed nanostructures, such as hexagonal, square, and honeycomb-like ncp arrays, and hexagonal close-packed (hcp) arrays. Interestingly, the 2D hexagonal and square ncp arrays can further bend and close to form vesicles with hexagonal and square ncp surface lattices, respectively. The free energy differences per particle of these 2D nanostructures with respect to the reference 2D hexagonal ncp nanostructure fall in the range of about -13.0 to 0.0 k_BT, which are low enough to allow reversible structural transitions between them over a convenient timescale.[22] Our work demonstrates that the template-free fabrication of 2D nanostructures is readily accessible through the rational design of soft Janus particles.

2 Model of soft triblock Janus particles

The pair wise interaction between soft triblock Janus particles is described by a soft and anisotropic attractive potential, based on the soft-particle model in dissipative particle dynamics[34] and the Kern–Frenkel model.[35] For simplicity, we use the interaction cutoff radius (r_c) as the unit of length, k_BT as the unit of energy, and choose the moment of inertia (I) and the mass (m) of the particle as the units, thus the time unit $\tau = \sqrt{mr_c^2/k_BT}$. The variables and parameters in the following will be given in reduced units. The proposed anisotropic potential is expressed as

$$U_{ij} = \begin{cases} \frac{\alpha_{ij}^{R}}{2}(1 - r_{ij})^2 - f^{\nu}\frac{\alpha_{ij}^{A}}{2}\left(r_{ij} - r_{ij}^2\right) & r_{ij} \le r_c \equiv 1.0 \\ 0 & r_{ij} > r_c, \end{cases} \quad (1)$$

where

$$f = \begin{cases} \cos\frac{\pi}{2}\left(\frac{\pi/2 - \theta_i'}{\pi/2 - \beta}\right)\cos\frac{\pi}{2}\left(\frac{\pi/2 - \theta_j'}{\pi/2 - \beta}\right) & \text{if } |\cos\theta_i| \le \cos\beta \\ & \text{and } |\cos\theta_j| \le \cos\beta \\ 0 & \text{otherwise.} \end{cases}$$

As illustrated in Fig. 1, the cyan parts of the particle surface represent the repulsive patches and the orange part represents the attractive middle band, and the directions of the repulsive patches on particles i and j are specified by unit vectors $\mathbf{n}_i$ and $\mathbf{n}_j$, respectively. θ_i is the angle between $\mathbf{n}_i$ and the interparticle vector $\mathbf{r}_{ji} = \mathbf{r}_j - \mathbf{r}_i$, and θ_j is the angle between $\mathbf{n}_j$ and $\mathbf{r}_{ij} = -\mathbf{r}_{ji}$, and then $\cos\theta_i = -\mathbf{n}_i\cdot\mathbf{r}_{ij}/r_{ij}$ and $\cos\theta_j = \mathbf{n}_j\cdot\mathbf{r}_{ij}/r_{ij}$. Here, $\theta_i' = \arccos(|\cos\theta_i|)$ and $\theta_j' = \arccos(|\cos\theta_j|)$. The size of the repulsive patches is described by Janus balance β, which is the half of the opening angle of the repulsive patches, and the fraction of the surface covered by the attractive middle band χ is related to β by the relation $\chi = 1 - 2\sin^2\left(\frac{\beta}{2}\right)$,[35] thus the increasing Janus balance β corresponds to the decreasing attractive middle band. In eqn (1), the parameters α_{ij}^{R} and α_{ij}^{A} are scaled by the unit of energy k_BT, the magnitude of α_{ij}^{R} controls the strength of repulsion, α_{ij}^{A} controls the strength of attraction between the attractive middle band, and ν controls the angular width of the attraction. Thus, both α_{ij}^{A} and ν control the flexibility of Janus particle aggregates. As shown in Fig. S1,† the distance dependence of U_{ij} presents explicitly weak attraction at a long range while $\theta_i = 90°$, and the strength of the attraction will decrease with decreasing θ_i. Therefore, it is clear that the side-by-side alignment of soft triblock Janus particles is energetically favorable.

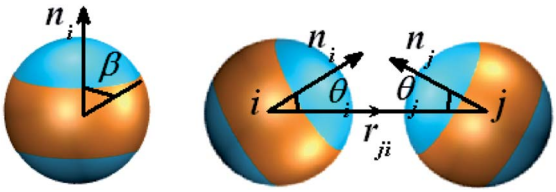

Fig. 1 Model of soft triblock Janus particles.

Our soft Janus particle model can be directly mapped onto experimental systems under different ambient conditions,[36,37] and has already been shown to successfully describe the self-assembly of soft one-patch Janus particles[36] and the ordered packing of soft triblock Janus particles.[37] As given in ref. 36 and 37, when $\theta_i = \theta_j = \pi/2$, eqn (1) becomes an isotropic potential with a shallow attractive well. Thus α_{ij}^{R} can be related to the linear elastic modulus of the particle, E, by $\alpha_{ij}^{R} = \pi E d^2/6$,[38,39] where d is the effective diameter of the soft Janus particle. The effective diameter d can be estimated by $d = (\alpha_{ij}^{R} + \alpha_{ij}^{A}/2)/(\alpha_{ij}^{R} + \alpha_{ij}^{A})$. If we define δ as the range of attraction relative to the effective diameter d, and $(1 + \delta)d = r_c$, then δ is also related to α_{ij}^{R} and α_{ij}^{A} by $\delta = \alpha_{ij}^{A}/(2\alpha_{ij}^{R} + \alpha_{ij}^{A})$. The energy minimum of the attractive potential at $r_{ij} = d$ gives $G = -U_{ij}^{min} = \alpha_{ij}^{A}(1 - d)/4$, where the adhesion energy G determines the association strength between particles. Thus the simulation parameters α_{ij}^{R} and α_{ij}^{A} can be fixed from experimentally measurable particle properties, including the elastic modulus E, the effective diameter d, and the adhesion energy G. The adhesion energy G determines the association strength between particles, and can be tuned by altering the salt concentration, pH, or temperature. In the simulations, changing the strength of attraction α_{11}^{A} corresponds to varying the adhesion energy G, and the corresponding relation between them is given in Table S1.†

The simulations are performed under NVT conditions (the number of particles, the volume, and the temperature are constant). The weak coupling Berendsen thermostat, which is stable, efficient, and simple to implement, is used to control the temperature at the target value.[36,37,40] Although the Berendsen thermostat is unable to generate a well defined ensemble (especially for small systems), it has been widely used in simulations because the approximation yields roughly correct results for most calculated properties for large systems on the order of thousands of atoms/molecules/particles.[40–43] We simulate systems of 2.4×10^4 particles in a $20 \times 20 \times 20$ cubic box with periodic boundary conditions. The number of Janus particles is $N_{solute} = 24\,000 \times \phi$, and the number of spherical solvent particles is $N_{solvent} = 24\,000 \times (1 - \phi)$ (ϕ is the concentration of Janus solute particles). In order to assess the system size effect and the reproducibility of the self-assembled

structures, larger systems with box size $40 \times 40 \times 40$ (1.92×10^5 particles) are also simulated with longer time from different initial configurations. The solute–solvent and solvent–solvent interactions follow the first term of eqn (1). A time step $\delta t = 0.002\tau$ is used. It should be noted that the coarse-grained model may lead to the reduction in degrees of freedom of solvent particles, and therefore, result in different entropies. But this problem may be partially solved by constructing effective coarse-grained potential which is designed to reproduce correct structure and thermodynamic properties of a given system at a specific condition.[34,36,38,39,44,45]

In the simulations, we choose $\alpha_{11}^{R} = \alpha_{22}^{R} = 396$ (1: Janus particle; 2: solvent particle), $\phi = 5\%$, and $\nu = 1/2$. If the reduced unit of length r_c in the model corresponds to 20 nm, the corresponding elastic modulus E of the particles is approximately equal to 4.0 MPa, which indicates that the Janus particles in our model are soft and deformable as compared to typical hard-sphere particles with modulus about 2.0 GPa.[36,37] Changing the repulsion strength α_{12}^{R} between Janus and solvent particles corresponds to varying the solvent condition. For simplicity, we keep athermal solvent condition with $\alpha_{12}^{R} = 396$.

3 Results and discussion

3.1 Self-assembly diagram of soft triblock Janus particles

Both the Janus balance, β, which characterizes the size of repulsive patches on a triblock Janus particle, and the strength of attraction G between Janus particles can be tuned by chemical modification experimentally. To clarify their cooperative influence on the self-assembled nanostructures, the self-assembly diagram of soft triblock Janus particles, obtained from a large number of simulations, is described in Fig. 2. Each of the simulations starts from an initially isotropic configuration. This diagram shows, in a large range of Janus balance and attraction strength, that the 2D single-layer nanostructures with various patterns can be formed. As shown in Fig. 2, when the Janus balance is not too small (*i.e.*, the attractive middle band is not too large), the 2D single-layer hexagonal ncp (sh-ncp) arrays can be observed in the cases with weak inter-particle attraction. If we continue increasing the adhesion energy G, which will result in a larger overlap between soft triblock Janus particles, 2D square ncp (s-ncp) arrays, stretched honeycomb-like (shc-ncp) arrays and honeycomb-like ncp (hc-ncp) arrays, and hcp arrays can be observed one by one. Meanwhile, we observe two coexisting structures of s-ncp arrays and shc-ncp arrays, and hc-ncp arrays and hcp arrays (as shown in Fig. S2†). Moreover, the 2D sh-ncp and s-ncp nanostructures are flexible, and with a proper choice of Janus balance and adhesion energy, they can close to form vesicles with sh-ncp (orange triangle symbols) and s-ncp (green square symbols) surface lattices, respectively. In order to estimate the size of these vesicles, we have performed five independent simulations from different initial configurations for each typical parameter set shown in Fig. 2, and the aggregation numbers of the obtained vesicles are all roughly in the range of 1100–1300 particles. As can be seen in Fig. 2 and S2,† this self-assembly diagram is not sensitive to Janus balance β, except in a very narrow region where multi-layer hexagonal

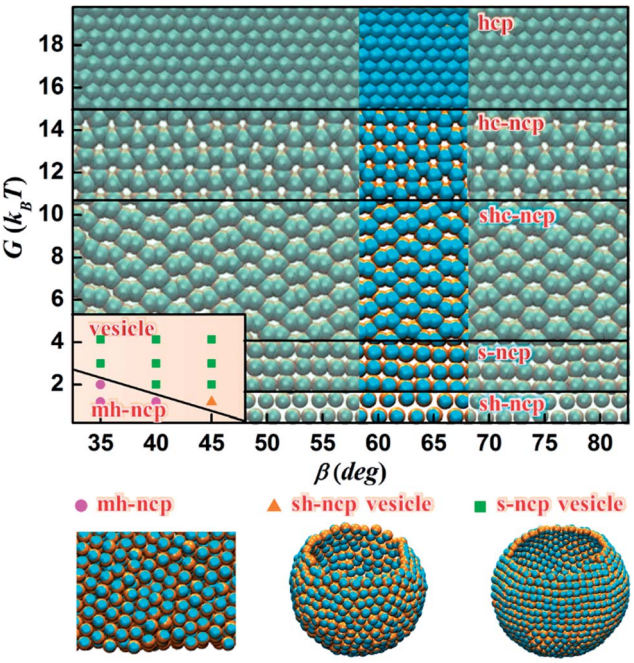

Fig. 2 Self-assembly diagram of soft triblock Janus particles in the G–β plane, the boundaries are drawn schematically to guide the eye. By properly tuning the Janus balance β and the adhesion energy G, soft triblock Janus particles can self-assemble into a number of fascinating ordered nanostructures, including multi-layer hexagonal ncp (mh-ncp) arrays, 2D single-layer hexagonal ncp (sh-ncp), square ncp (s-ncp), stretched honeycomb-like ncp (shc-ncp), and honeycomb-like ncp (hc-ncp) arrays, hcp arrays, and the vesicles with the sh-ncp and s-ncp surface lattices.

ncp (mh-ncp) arrays or vesicles emerge. The finite size effect on the self-assembly diagram in Fig. 2 is negligible (as shown in Fig. S3†), and all of these self-assembled nanostructures are reproducible in our simulations. Looking ahead to possible applications, these 2D ordered ncp nanostructures, especially shc-ncp and hc-ncp nanostructures with the hydrophobic holes, offer the potential for selective transports.[22] Furthermore, these 2D ordered ncp nanostructures are soft and flexible, which provides the potential in coating curved substrates[25] and soft-electronic and optical devices.[26,27] The vesicles with the sh-ncp and s-ncp surface lattices may be used as the vehicles for drug and biomolecule delivery and release.[46]

In order to provide evidence of different typical 2D ordered nanostructure arrays in our simulations, we calculate the radial distribution function $g(r)$ and the distribution $N(s)$ of the number of contacts between attractive middle bands per Janus particle s,[36,37] as shown in Fig. 3a and b, respectively. As demonstrated in Fig. 3, a doublet between 1.0 and 1.7 appears and $N(s)$ shows a narrow distribution at $s = 6$, which can be taken as the clear evidence of the sh-ncp arrays in Fig. 2. For the s-ncp arrays in Fig. 2, the relative positions of the first two peaks (at about 0.62 and 0.88) of $g(r)$ are $1 : \sqrt{2}$, and $N(s)$ shows a narrow distribution at $s = 8$. For the hc-ncp arrays, Janus particles pack more closely to form a regular hexagon, thus the relative positions of the first two peaks (at about 0.42 and 0.73) of $g(r)$ are $1 : \sqrt{3}$, and $N(s)$ shows an apparent distribution at $s =$

3. For the shc-ncp arrays, the regular hexagon is partially stretched, the first peak at about 0.42 splits into two peaks, as shown in Fig. 3a. Furthermore, as can be seen in Fig. 3a, the main peaks of these ordered nanostructure arrays gradually move toward smaller values of r, which suggests that the deformability and overlap of Janus particles are larger and larger with the increase of G. Thus, the obtained hcp arrays are more close-packed than the sh-ncp arrays, as shown in Fig. S4.†

3.2 Role of particle softness

The most possible 2D packing pattern for hard triblock Janus particles with the attractive middle band is a close-packed hexagonal monolayer structure. But for soft triblock Janus particles with the attractive middle band, various exotic non-close-packed 2D structures emerge due to the featured particle softness. Take the case with Janus balance $\beta = 60^\circ$ as an example, we monitor the center-to-center distances of soft triblock Janus particles in typical self-assembled nanostructures in the top panel of Fig. 4, through the calculation of the radial distribution function $g(r)$ in Fig. 3. With increasing adhesion energy G, the non-close-packed sh-ncp, s-ncp, hc-ncp, and close-packed hcp nanostructures are observed in turn, and the center-to-center distances of Janus particles become smaller and smaller, suggesting that the soft triblock Janus particles can deform and even largely overlap with each other on increasing the adhesion energy G. We find that the ratio between the inter-particle distance and the reduced unit of length r_c in the model (h) is not sensitive to

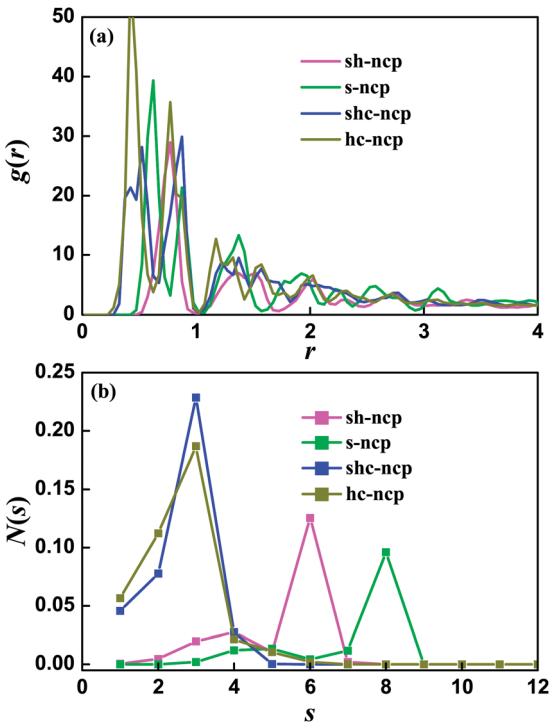

Fig. 3 (a) The radial distribution function $g(r)$ and (b) the distribution $N(s)$ of the number of contacts between attractive middle bands per Janus particle s in typical self-assembled nanostructures shown in Fig. 2. The distributions $N(s)$ have been normalized so that $\sum_s sN(s) = 1$.

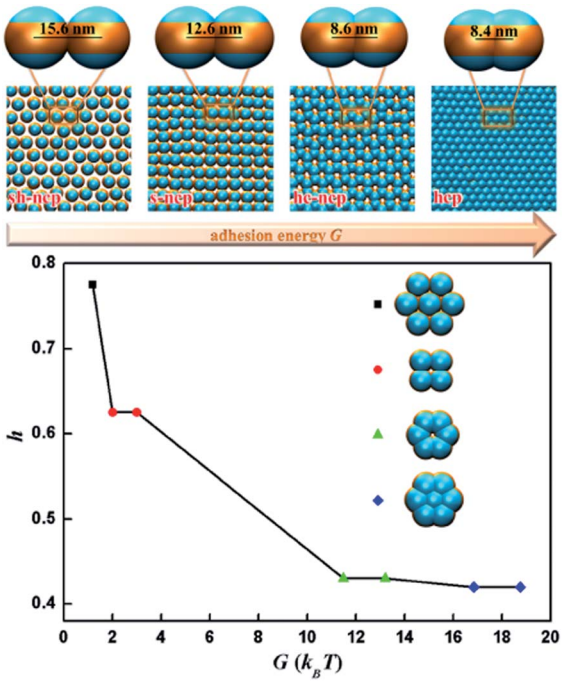

Fig. 4 The center-to-center distances of soft triblock Janus particles in typical self-assembled nanostructures with increasing adhesion energy G (top panel), and the dependence of the ratio between the inter-particle distance and the reduced unit of length r_c in the model h on the adhesion energy G (bottom panel).

Janus balance β in a large range of Janus balance value ($\beta \in [50^\circ, 80^\circ]$) at the same adhesion energy. It suggests that in experiments, the key issue is to keep the Janus particle suitably soft, therefore they can overlap with each other and selectively form 2D structures with characteristic patterns indicated by the factor h. In the bottom panel of Fig. 4, we also show the regions of G and h where the specific ordered patterns can be observed. Note that the factor h can be easily tuned either by changing the inter-particle adhesion energy or by controlling the particle modulus at an experimentally accessible Janus particle diameter. Thus in contrast to hard Janus colloidal particles, the softness of triblock Janus particles plays a deterministic role in the formation of these 2D ordered non-close-packed nanostructures.

3.3 The stability of 2D self-assembled nanostructures

The relative stability of these 2D nanostructures can be efficiently evaluated through calculating their free energy differences with respect to the reference nanostructure. As we know, for hard crystalline solids, the Einstein crystal is an appropriate reference state, whose absolute free energy can be accurately calculated, one could utilize thermodynamic integration to calculate the free energy at different state points.[47,48] However, in self-assembling soft matter systems, the molecules diffuse and are not constrained to be at ideal positions, the analog of the Einstein crystal is absent. Therefore, the simulation techniques for calculating the absolute free energy of hard crystals cannot be easily generalised to self-assembling soft matter systems.[47,48] Nevertheless, the free energy differences of the self-

assembling systems between the reference state and the state of interest can also be calculated by thermodynamic integration, if the integration path from the initial to final state is reversible.[49]

As indicated above, varying the strength of attraction α_{11}^{A} (*i.e.* the adhesion energy G) corresponds to altering the salt concentration, pH, or temperature in experiments. Thus, the annealing-like process of gradually increasing α_{11}^{A} is equivalent to thermal annealing or solvent annealing in experiments. As shown in Fig. S5 and S6,† the annealing-like processes from sh-ncp arrays to s-ncp arrays, to shc-ncp arrays, to hc-ncp arrays, and finally to hcp arrays are reversible because of almost no discontinuity and hysteresis.[10] So the free energy differences of these ordered 2D nanostructure systems with respect to the reference 2D sh-ncp nanostructure system can be calculated by thermodynamic integration.[49] The integrating equation is expressed as $F(\alpha_{11,\mathrm{ordered}}^{A}) - F(\alpha_{11,\mathrm{ref}}^{A}) = \int_{\alpha_{11,\mathrm{ref}}^{A}}^{\alpha_{11,\mathrm{ordered}}^{A}} d\alpha_{11}^{A} \left\langle \frac{\partial U(\alpha_{11}^{A})}{\partial \alpha_{11}^{A}} \right\rangle_{\alpha_{11}^{A}}$, where $\langle \cdots \rangle_{\alpha_{11}^{A}}$ denotes an ensemble average for a system with a potential function $U(\alpha_{11}^{A})$.[49] Fig. 5 shows the free energy differences per particle ΔF_p for representative 2D ordered nanostructures with 2D sh-ncp nanostructure as the reference measured with the increasing rate of $\Delta\alpha_{11}^{A} = 2.75$ per 8×10^6 time step. All the free energy differences per particle of these 2D structures fall in the range of -13.0 to 0.0 k_BT, which are low enough to allow spontaneous formation of these 2D ordered nanostructures and observe reversible structural transitions between them over a convenient timescale.[22] This nontrivial result guarantees controllable response if the 2D ordered membrane is used as a stimuli-responsive separation device. Therefore, colloidal building blocks with tunable deformability and directional attraction give access to a rich variety of novel 2D nanostructures.

4 Conclusions

In summary, we have proposed a simple and novel strategy to achieve template-free fabrication of diverse 2D ordered nanostructures with the aid of the deformable and anisotropic characteristics of soft triblock Janus particles. The attraction strength between attractive middle bands and the Janus balance coordinate to generate a number of fascinating 2D ordered non-close-packed nanostructures, including the exotic vesicle structures with hexagonal and square ncp surface lattices. The free energy differences per particle of these 2D nanostructures are low enough to allow the formation of these 2D nanostructures and observe the reversible structural transitions between them. It is clear that the interplay between particle softness and controllable directional attraction plays a dominant role in creating 2D ordered ncp nanostructures. These 2D ordered nanostructures with soft and deformable characteristics may have great potential in selective transport, coating curved substrates, and soft-electronic and optical devices. The soft triblock Janus particles in our model are within the reach of today's experimental capabilities.[13,17,28–33] Our work paves the way for the experimental realization of 2D well-ordered nanostructures, and offers a new direction for the creation of novel colloidal nanostructures without any template.

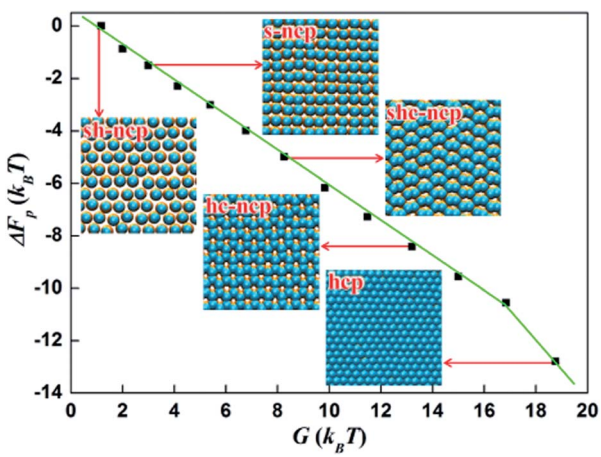

Fig. 5 The free energy differences per particle ΔF_p for representative 2D ordered nanostructures with respect to the reference 2D sh-ncp nanostructure.

Acknowledgements

This work is subsidized by the National Basic Research Program of China (973 Program, 2012CB821500). The authors also appreciate the financial supports from the National Science Foundation of China (21104084, 21122407, 21025416).

References

1 K. Baek, *et al.*, *J. Am. Chem. Soc.*, 2013, **135**, 6523.
2 J. Zhang, Y. Li, X. Zhang and B. Yang, *Adv. Mater.*, 2010, **22**, 4249.
3 P. Jiang and M. J. McFarland, *J. Am. Chem. Soc.*, 2005, **127**, 3710.
4 N. Vogel, *et al.*, *Adv. Funct. Mater.*, 2011, **21**, 3064.
5 J.-T. Zhang, *et al.*, *Angew. Chem., Int. Ed.*, 2012, **51**, 6117.
6 X. Yan, *et al.*, *J. Am. Chem. Soc.*, 2005, **127**, 7688.
7 J. P. Hoogenboom, *et al.*, *Nano Lett.*, 2004, **4**, 205.
8 S. Acharya, J. P. Hill and K. Ariga, *Adv. Mater.*, 2009, **21**, 2959.
9 S. Yang and Y. Lei, *Nanoscale*, 2011, **3**, 2768.
10 Z. Zhang and S. C. Glotzer, *Nano Lett.*, 2004, **4**, 1407.
11 S. C. Glotzer and M. J. Solomon, *Nat. Mater.*, 2007, **6**, 557.
12 A. B. Pawar and I. Kretzschmar, *Macromol. Rapid Commun.*, 2010, **31**, 150.
13 A. Walther and A. H. E. Müller, *Soft Matter*, 2008, **4**, 663.
14 J. Du and R. K. O'Reilly, *Chem. Soc. Rev.*, 2011, **40**, 2402.
15 M. Lattuada and T. A. Hatton, *Nano Today*, 2011, **6**, 286.
16 J. Hu, *et al.*, *Chem. Soc. Rev.*, 2012, **41**, 4356.
17 A. Walther and A. H. E. Müller, *Chem. Rev.*, 2013, **113**, 5194.
18 F. Sciortino, A. Giacometti and G. Pastore, *Phys. Rev. Lett.*, 2009, **103**, 237801.
19 Q. Chen, *et al.*, *Science*, 2011, **331**, 199.
20 J. Yan, *et al.*, *Science*, 2012, **491**, 578.
21 F. Romano and F. Sciortino, *Nat. Commun.*, 2012, **3**, 975.
22 Q. Chen, S. C. Bae and S. Granick, *Nature*, 2011, **469**, 381.
23 Q. Chen, *et al.*, *J. Am. Chem. Soc.*, 2011, **133**, 7725.
24 F. Romano and F. Sciortino, *Nat. Mater.*, 2011, **10**, 171.
25 S. Fujii, *et al.*, *Angew. Chem., Int. Ed.*, 2012, **51**, 9809.

26 S. R. Forrest, *Nature*, 2004, **428**, 911.
27 J. A. Rogers, T. Someya and Y. Huang, *Science*, 2010, **327**, 1603.
28 A. H. Gröschel, *et al.*, *J. Am. Chem. Soc.*, 2012, **134**, 13850.
29 A. H. Gröschel, *et al.*, *Nat. Commun.*, 2012, **3**, 710.
30 D. Suzuki, S. Tsuji and H. Kawaguchi, *J. Am. Chem. Soc.*, 2007, **129**, 8088.
31 T. M. Hermans, *et al.*, *Nat. Nanotechnol.*, 2009, **4**, 721.
32 V. Percec, *et al.*, *Science*, 2010, **328**, 1009.
33 Y. Liu, C. Yu, H. Jin, B. Jiang, X. Zhu, Y. Zhou, Z. Lu and D. Yan, *J. Am. Chem. Soc.*, 2013, **135**, 4765.
34 R. D. Groot and P. B. Warren, *J. Chem. Phys.*, 1997, **107**, 4423.
35 N. Kern and D. Frenkel, *J. Chem. Phys.*, 2003, **118**, 9882.
36 Z.-W. Li, Z.-Y. Lu, Z.-Y. Sun and L.-J. An, *Soft Matter*, 2012, **8**, 6693.
37 Z.-W. Li, Z.-Y. Lu, Y.-L. Zhu, Z.-Y. Sun and L.-J. An, *RSC Adv.*, 2013, **3**, 813.
38 R. D. Groot and S. D. Stoyanov, *Phys. Rev. E: Stat., Nonlinear, Soft Matter Phys.*, 2008, **78**, 051403.
39 R. D. Groot and S. D. Stoyanov, *Soft Matter*, 2010, **6**, 1682.
40 H. J. C. Berendsen, J. P. M. Postma, W. F. van Gunsteren, A. DiNola and J. R. Haak, *J. Chem. Phys.*, 1984, **81**, 3684.
41 B. Fodi and R. Hentschke, *J. Chem. Phys.*, 2000, **112**, 6917.
42 A. Mudi and C. Chakravarty, *Mol. Phys.*, 2004, **102**, 681.
43 G. Bussi, D. Donadio and M. Parrinello, *J. Chem. Phys.*, 2007, **126**, 014101.
44 H. S. Ashbaugh, H. A. Patel, S. K. Kumar and S. Garde, *J. Chem. Phys.*, 2005, **122**, 104908.
45 S. Jain, S. Garde and S. K. Kumar, *Ind. Eng. Chem. Res.*, 2006, **45**, 5614.
46 J. M. Fletcher, *et al.*, *Science*, 2013, **340**, 595.
47 M. Müller and K. C. Daoulas, *J. Chem. Phys.*, 2008, **128**, 024903.
48 Y. Norizoe, K. C. Daoulas and M. Müller, *Faraday Discuss.*, 2010, **144**, 369.
49 D. Frenkel and B. Smit, *Understanding Molecular Simulation: From Algorithms to Applications*, Academic Press, San Diego, 2nd edn, 2002.